SRNL-STI-2010-00204

Layered perovskite $PrBa_{0.5}Sr_{0.5}Co_2O_{5+\delta}$ as high performance cathode for solid oxide fuel cells using proton conducting electrolyte

Fei Zhao [a], Kyle Brinkman [b], Fanglin Chen [a], *

[a] Department of Mechanical Engineering, University of South Carolina, 300 Main Street, Columbia, SC 20208, USA

[b] Savannah River National Laboratory (SRNL), Materials Science & Technology Directorate, Aiken, SC 29808, USA

* Corresponding Author

(Tel.) 803-777-4185; (fax) 803-777-0106

(E-mail): chenfa@cec.sc.edu

Abstract

The layered perovskite $PrBa_{0.5}Sr_{0.5}Co_2O_{5+\delta}$ (PBSC) was investigated as a cathode material for a solid oxide fuel cell using a proton-conducting electrolyte based on $BaCe_{0.7}Y_{0.2}Zr_{0.1}O_{3-\delta}$ (BCYZ). The sintering conditions for the PBSC-BCYZ composite cathode were optimized resulting in the lowest area-specific resistance and apparent activation energy obtained with the cathode sintered at 1200°C for 2h. The maximum power densities of the PBSC-BCYZ/BZCY/NiO-BCYZ cell were 0.179, 0.274, 0.395, and 0.522 Wcm^{-2} at 550, 600, 650, and 700°C, respectively with a 15μm thick electrolyte. A relatively low cell interfacial polarization resistance of 0.132 Ωcm^2 at 700 °C indicated that the PBSC-BCYZ could be a good cathode candidate for intermediate temperature SOFCs with proton-conducting electrolyte.

Keywords: Solid oxide fuel cell; Proton conductor; Layered perovskite; Cathode

1. Introduction

Solid oxide fuel cells (SOFCs) are considered to be one of the most promising energy conversion devices due to their high energy conversion efficiency, ability to use low cost non-precious metal catalysts, fuel flexibility and system compactness compared to other types of fuel cells [1]. However, SOFCs are currently not economically competitive due to problems associated mainly with high temperature (>800°C) operation, including performance degradation of cell components resulting from high temperature oxidation, corrosion, chemical interdiffusion and reaction, structural failure due to creep deformation, high thermal stress at the interfaces of the various SOFC components, as well as high cost of the overall SOFC system [2, 3]. One approach to cost reduction is to decrease the SOFC operating temperature below 700^{o}C so that inexpensive metals can be used for interconnects, heat exchangers, manifolding and other structural components of the SOFC system [4].

A lower operating temperature would ensure greater overall system stability due to a reduction in the thermal stresses in the active ceramic structures, leading to a longer expected lifetime for the SOFC system. A decrease in the operating temperature is expected to improve the SOFC durability since oxidation, corrosion, chemical interdiffusion and creep deformation will be reduced at reduced operating temperatures. In addition, lowering the SOFC operation temperature can also offer quick start-up ability, which in turn can enable their use in applications such as transportable power sources and auxiliary power units for automobiles.

The SOFCs using proton conducting ceramics are currently under consideration for applications at intermediate temperatures (500-800^{o}C). In contrast to oxygen-ion conducting SOFCs, proton-conducting SOFCs have lower reaction activation energy and form water in the cathode chamber, which can avoid problems associated with fuel dilution [5]. Considerable efforts have been made to develop proton conductors with high conductivity and stability such as $BaZr_yCe_{0.8-y}Y_{0.2}O_{3-\delta}$ which is a leading electrolyte material for intermediate temperature applications [6-8]. Despite the advantages of proton conducting ceramics at intermediate temperature, a major concern with reduced temperatures is the deterioration of cathode performance. This behavior originates from poor cathodic electrochemical activity for oxygen reduction and high cathode concentration overpotential due to water generation in the cathode chamber.

The development of proper cathode materials for protonic ceramic membrane fuel cells in order to improve materials compatibility and reduce costs remains a challenge. Noble metals (Pt, Pd) as well as simple perovskite-type mixed ionic–electronic conductors (MIEC) such as $La_{0.6}Sr_{0.4}CoO_{3-\delta}$, $Sm_{0.5}Sr_{0.5}CoO_{3-\delta}$, $La_{0.5}Sr_{0.5}FeO_{3-\delta}$ and $Ba_{0.5}Sr_{0.5}Co_{0.8}Fe_{0.2}O_{3-\delta}$ have been extensively studied as cathodes for IT-SOFCs [9, 10]. However, not much attention has been paid to layered perovskite materials. Recently, cation-ordered $LnBaCo_2O_{5+\delta}$ (Ln=La, Pr, Nd, Sm, Gd, and Y) have been systemically investigated as cathodes for oxygen-ion conductor SOFCs [11]. Among the various layered $LnBaCo_2O_{5+\delta}$ oxides, $PrBaCo_2O_{5+\delta}$ has the highest bulk diffusion coefficient, surface exchange coefficient and the lowest area specific polarization resistance for SOFCs based on samarium-doped ceria electrolyte. These results indicate that layer-structured oxides are a promising alternative material for SOFC cathodes [12].

The oxygen ion diffusivity and surface exchange coefficients of $PrBaCo_2O_{5+\delta}$ (PBC) at 350°C are about 10^{-5} cm^2 s^{-1} and 10^{-3} cm s^{-1}, respectively, which are 2–3 orders of magnitude higher than those of $La_{0.5}Sr_{0.5}CoO_{3+\delta}$ [13]. In addition, the ASR value of a composite cathode using PBC on a $Ce_{0.9}Gd_{0.1}O_{2-\delta}$ electrolyte was found to be as low as $0.15\Omega cm^2$ at 600°C. More recently, Kim and coworkers reported a novel layered $PrBa_{0.5}Sr_{0.5}Co_2O_{5+\delta}$ (PBSC) perovskite that demonstrated advanced electrochemical properties as a cathode in an oxygen ion SOFC based on doped ceria electrolyte used in intermediate temperature regimes. Consequently, PBSC can be potentially utilized as a cathode material for IT-SOFC applications due to its unique combination of superior catalytic activity and similar thermal expansion coefficient compared to other SOFC components [14]. It is anticipated that enhanced SOFC cell performance may be obtained by using a composite cathode consisting of PBSC and $BaCe_{0.7}Y_{0.2}Zr_{0.1}O_{3-\delta}$ (BCYZ).

The objective of this study is to develop a high performance proton-conducting SOFC by combining a layered perovskite PBSC cathode and thin film BZCY electrolyte. In this work, the electrochemical performance of the PBSC–BZCY composite cathode was evaluated using symmetrical cells. In addition, a suspension-coating technique was employed to fabricate the BCYZ thin film and the single cell performance with PBSC-BCYZ composite cathode was also investigated at a range of temperatures.

2. Experimental

2.1 Powder preparation

The cathode and electrolyte powders were synthesized by a modified Pechini process. The starting materials consisting of $Pr(NO_3)_3{\cdot}6H_2O$ (Alfa Aesar), $Ba(NO_3)_2$ (Alfa Aesar, 99.95%), $Sr(NO_3)_3$(Alfa Aesar, 99.5%), and $Co(NO_3)_2{\cdot}6H_2O$ (Alfa Aesar, 99.9%) as metal precursors. In addition, EDTA (Ethylenediaminetetraacetic acid, Alfa Aesar, 99%) and citric acid (Alfa Aesar, 99%) were used as chelating and complexing agents, respectively for the $PrBa_{0.5}Sr_{0.5}Co_2O_{5+\delta}$ synthesis. Ammonium hydroxide (Sigma-Aldrich, NH_3 content 28.0 to 30.0%) was added to promote the dissolution of EDTA in deionized water. An appropriate amount of barium nitrate was first dissolved in deionized water. An aqueous solution of EDTA and ammonia (pH~9) was then added drop-wise to the barium solution. The mixture was kept at 50^oC with mild continuous stirring until a clear solution was obtained. An aqueous solution containing stoichiometric amounts of praseodymium, strontium and cobalt salts was subsequently slowly added to the barium nitrate solution. Finally, an appropriate amount of citric acid was added (citric acid : metal nitrates : EDTA molar = 1.5 : 1 : 1) and the final solution was stirred at room temperature for 24 h. Water was then slowly evaporated on a hot plate and the resulting brown gel was dried at 300^oC. The dried ashes were then placed in a muffle furnace and treated at 1100^oC for 6 hour in air to remove the residual organic residue. The $BaCe_{0.7}Y_{0.2}Zr_{0.1}O_{3-\delta}$ electrolyte powders were also fabricated by the similar process with $Ba(NO_3)_2$, $Ce(NO_3)_3{\cdot}6H_2O$, $Y(NO_3)_3{\cdot}6H_2O$, and $ZrO(NO_3)_3{\cdot}2H_2O$ as the precursor materials and then calcined at 1100^oC for 2h in air.

2.2 Cell fabrication

As-prepared BCYZ powders were mixed and ground in a mortar and pestle and uni-axially pressed into pellets at 400 MPa, followed by sintering at 1450^oC for 5 hours in air. Symmetrical electrode configuration was used to measure the electrode electrochemical performance. For the composite cathode, 50 wt% PBSC and BCYZ powders were mixed homogeneously and made into slurry with a commercial binder (V-006, Heraeus). The slurry was screen-printed onto both sides of the BCYZ pellets, followed by sintering at different temperatures to obtain symmetrical cathode cells.

The anode-supported BCYZ half cells were prepared by a suspension-coating method. Substrates consisting of 65 wt.% NiO (Sigma-Aldrich, 99.99%) and 35 wt.% BCYZ were fabricated with die pressing. NiO and BCYZ were pre-mixed and ball-milled for 24 h. The mixed powders were pressed uniaxially into pellets with a diameter of 15 mm, followed by firing at 800 °C for 2 h to form porous substrates. BCYZ electrolyte films were deposited on the as-prepared substrates with a suspension-coating method. BCYZ powders and dispersants were mixed with absolute ethanol and ball-milled for 48 h to form a stable suspension with 10 wt.% solid content. The suspension was then drop-coated onto the substrates with an injector. The electrolyte thickness was controlled by the amount of BCYZ suspension coated on the substrate surface. To avoid cracks formation as induced from evaporation of the organics, the film was dried in an ethanol ambient at room temperature. The electrolyte coated anode substrates were then co-fired at 1400^{o}C for 5h to form a dense electrolyte film. Subsequently, PBSC-BCYZ cathode slurry was then screen-printed onto the BCYZ electrolyte, followed by sintering at 1200^{o}C for 2h to form a PBSC-BCYZ/BCYZ/NiO-BCYZ cell. The apparent area of the cathode is 0.3cm^2.

2.3 Cell test

Silver paste (Heraeus, component metallization C8809) was painted on the cathode, and then fired at 500^{o}C for 1 h to form a porous silver current collector. The single cell was attached and sealed on an alumina tube using the silver paste. The cell was heated to 600 ^{o}C with hydrogen flowing to the anode and NiO was reduced to Ni in situ. The cell was stabilized at 550 ^{o}C for 2 h. Electrochemical tests were performed with the humidified hydrogen as fuel and ambient air as oxidant.

2.4 X-ray diffraction measurement, microstructure and performance characterization.

The X-ray diffraction (XRD) patterns of the prepared PBSC, BCYZ powders and PBSC-BCYZ composite cathode were obtained in a Mini X-ray diffractometer using Cu Kα radiation (λ=0.15418 nm), employing a scanning rate of 10 °/min in the 2θ range of 20 to 80°. The data were matched with the reference data for the identification of crystal structures. The microstructures of the symmetrical half-cell and single cell were investigated using a scanning electron microscopy (SEM, FEI Quanta-XL 30 model). Cathode electrochemical performance and area-specific resistances (ASRs) were evaluated using the symmetrical cells at open-circuit voltage in air as a function of temperature between 550 and 800°C with a temperature increment of 50°C. AC impedance characteristics were measured with an electrochemical station (Versa STAT3-400, METEK) over a frequency range of 0.01 Hz to 1 MHz and a 10 mV ac perturbation. The cathode polarization was determined from the differences of the low- and high-frequency intercept on the impedance curves and then divided by 2.

3. Results and discussion

3.1 Phase formation

XRD results of pure PBSC, BCYZ powder and PBSC-BCYZ composite cathodes are shown in Fig. 1. The PBSC and BCYZ oxides prepared by the modified EDTA-citrate combustion method after calcination at 1100^{o}C for 6h in air are all identified as single phases. In the XRD result presented in Fig. 1 (a), there are no any peaks attributable to impurities and the structure of PBSC is identified as tetragonal, which is in good agreement with the literature result [15]. The as-prepared powder of BCYZ exhibits a single perovskite phase structure after calcination at 1100^{o}C for 6h in air. Special attention should be given to the phase reaction between PBSC and BCYZ in the cathode fabrication process and its potential influence on the cell performance. Mixtures of PBSC and BCYZ were heat-treated for 2 h at various temperatures between 900 and 1200°C and the phase composition was analyzed. The results shown in Fig. 1 (c, d) reveal that no reaction between PBSC and BCYZ occurred at 1200 °C, indicating that the layered perovskite PBSC is chemically compatible with the BCYZ electrolyte. The PBSC therefore can be used as the cathode in direct contact with the BCYZ electrolyte for IT-SOFCs.

3.2 Effect of sintering temperature on cathode performance

To investigate the effect of sintering temperature on the performances of the

PBSC-BCYZ composite cathodes, cathode specimens were sintered at 900, 1100 and 1200°C in air for 2h. The ASRs of PBSC-BCYZ composite cathodes with respect to various sintering temperatures are summarized in Fig. 2. From these results, it can be seen that the PBSC-BCYZ composite cathode sintered at 1200°C exhibited the lowest ASR values of $0.197\Omega cm^2$ at 800°C, $0.551\Omega cm^2$ at 700°C, and $1.669\Omega cm^2$ at 600°C, which were almost one order of magnitude lower than those of PBSC-BCYZ cathode sintered at 900°C for 2h. The apparent activation energies (E_a) of PBSC-BCYZ cathodes sintered at different temperatures were also shown in Fig. 2. The E_a values of PBSC-BCYZ cathodes sintered at 900°C, 1100°C, and 1200°C are $137.62 kJmol^{-1}$, $105.33 kJmol^{-1}$, and $82.33 kJmol^{-1}$, respectively. Low apparent activation energy indicated that PBSC-BCYZ cathode sintered at 1200°C had less chemical barrier for oxygen reduction, which resulted in a low ASR value [1, 9].

One possible origin of the low ASR value of the material sintered at 1200°C is microstructural enhancement. The fracture cross sections of the PBSC-BCYZ composite cathodes revealed the microstructure of the optimal sintering temperature (Fig. 3). Compared with the composite cathode sintered at 1200°C (Fig. 3 (b) and (d)), the PBSC particles sintered at 900°C for 2h (Fig. 3 (a)) were smaller, however, the microstructure of the cathode sintered at 1200°C was more porous. The more porous electrode can result in reduced mass transport losses [16]. It is well known that a composite cathode can not only reduce the thermal expansion but also minimize the discontinuities in the cathode. Employing an elevated sintering temperature can increase the triple-phase-boundary contact of a composite cathode [1, 9, 17]. As shown in Fig. 3(c), the cathode sintered at 900°C showed relatively poor adhesion at the cathode/electrolyte interface and was easily peeled off. Better adhesion was observed when the cathodes were sintered at 1200°C (Fig. 3(d)). At 900°C, the temperature was not high enough to result in a structure of sufficient particle necking for good contact and adhesion. At higher temperatures, particle necking resulted in improved adhesion and more porous microstructure. Consequently, the results indicate that a sintering temperature of 1200°C seems to provide a good balance between the conflicting electrode requirements of maintaining a porous, relatively high surface-area structure while at the same time providing a strong and well-bonded interface with adequate adhesion. It should be noted that the sintering temperature might be further optimized by increasing the sintering temperature to obtain a lower ASR and better interfacial adhesion.

3.3 Cell performance

The performance of PBSC-BCYZ composite cathode for proton-conductor IT-SOFCs, were evaluated by measuring the polarization characteristics of the cells from 550 to 700^{o}C with humidified hydrogen (~3% H_2O) as fuel as shown in Fig. 4. Maximum power densities of 0.179, 0.274, 0.395, and 0.522 Wcm^{-2} with the OCV values of 1.117, 1.092, 1.063, and 1.033V were obtained at 550, 600, 650, and 700^{o}C, respectively. These initial results suggest that the cell performance is very promising and the electrolyte membrane is sufficiently dense. In addition, the cell with a PBSC-BCYZ composite cathode fabricated in this study demonstrated higher power densities than those (0.128, 0.245, and 0.377 Wcm^{-2} at 550, 600, and 650°C, respectively) reported using a layered perovskite $SmBa_{0.5}Sr_{0.5}Co_2O_{5+\delta}$ cathode measured at or below 650°C [18]. to the enhanced performance is thought to arise from a denser electrolyte used in this study and the relatively low interfacial polarization resistance. Fig. 5 displays the impedance spectra of the cell measured under open-circuit conditions at different temperatures. The high frequency intercept corresponds to the ohmic resistance of the cell (R_o), while the low frequency intercept corresponds to the total resistance of the cell (R_t). Therefore, the difference between the high frequency and low frequency intercepts with the real axis represents the total interfacial polarization resistance (R_p) of the cell, including the cathode–electrolyte interfacial resistance and the anode–electrolyte interfacial resistance [9]. As expected, the increase of the measuring temperature resulted in a significant reduction of the interfacial polarization resistances as shown in Fig. 6, typically from 1.359 Ωcm^2 at 550°C to 0.132 Ωcm^2 at 700°C. The low polarization resistances indicated that PBSC-BCYZ composite cathode was a good candidate for operation at 700°C. As shown in Fig. 6, R_t is mainly dominated by R_p at or below 600°C, however, above 600°C, R_t is mainly dominated by R_o. Further analysis shows that the ratio of R_p to R_t decreases with the increase in operating temperature, from 67% at 550°C to 29% at 700°C, indicating that the cell performance is significantly limited by R_p at low temperatures. Compared to the fuel cell with a uniform anode and electrolyte but with other layered perovskite cathode materials such as $PrBaCuFeO_{5+\delta}$ [19], $GdBaCo_2O_{5+\delta}$

[20], and $SmBaCo_2O_{5+\delta}$ [21], the interfacial resistance of PBSC is lower than these common alternative cathode materials at temperatures below 700 ^{o}C. The improvement might be due to the high bulk diffusion coefficient and surface exchange coefficient. The results confirm that PBSC-BCYZ may be a promising alternative cathode for intermediate-temperature SOFCs using proton conductor as an electrolyte.

The cross-section micrograph of the single cell after the electrochemical tests is provided in Fig. 7. As shown in Fig. 7(a), the dense BZCY membrane (ca. 15μm) indicates that the drop-coating technique was successful. Compared with other thin film deposition technologies such as co-pressing [22], screen-printing [23] and gel-casting [24], the drop-coating technology is a simple and effective way to obtain a dense membrane. Fig. 7(b) shows that the PBSC-BCYZ cathode has a uniform porous microstructure, resulting in low interfacial polarization resistance and high electrochemical performance.

4. Conclusions

The layered perovskite $PrBa_{0.5}Sr_{0.5}Co_2O_{5+\delta}$ (PBSC) was synthesized by a modified Pechini process and characterized as a cathode for proton-conducting IT-SOFCs using $BaCe_{0.7}Y_{0.2}Zr_{0.1}O_{3-\delta}$ (BCYZ) as the electrolyte. The sintering conditions for the PBSC-BCYZ composite cathode were optimized. The lowest area-specific resistance and apparent activation energy were obtained with the cathode sintered at 1200°C for 2h. Cells with the optimized cathode and dense BCYZ electrolyte membrane showed very promising performance. The maximum power densities of the

PBSC-BCYZ/BCYZ/NiO-BCYZ cell with a 15μm thick electrolyte were 0.179, 0.274, 0.395, and 0.522 Wcm^{-2} at 550, 600, 650, and 700°C, respectively. A relatively low interfacial polarization resistance of 0.132 Ωcm^2 at 700 °C indicated that the PBSC-BCYZ could be a good cathode candidate for SOFCs using proton-conducting BCYZ electrolyte.

Acknowledgements

The financial support of the Department of Energy NEUP (award no. 09-510) and the South Carolina Universities Research and Education Foundation (award no. 09-155) is acknowledged gratefully. The SRNL LDRD program is acknowledged for the support of electronic ceramics for energy conversion applications.

References

[1] N.Q. Minh, J. Am. Ceram. Soc. 76 (1993) 563.

[2] B.C.H. Steele, A. Heinzel, Nature 414 (2001) 345.

[3] P. Singh, N. Minh, Int. J. Appl. Ceram. Technol. 1 (2004) 5.

[4] Q.L. Liu, K.A. Khor, S.H. Chan, J. Power Sources 161 (2006) 123.

[5] H. Iwahara, Solid State Ionics 86-88 (1996) 9.

[6] K.D. Kreuer, Annu. Rev. Mater. Res. 33 (2003) 333.

[7] K. Xie, R.Q. Yan, Y.Z. Jiang, X.Q. Liu, G.Y. Meng, J. Membrane Science 325 (2008) 6.

[8] Y.M. Guo, Y. Lin, R. Ran, Z.P. Shao, J. Power Sources 193 (2009) 400.

[9] S.B. Adler, Chem. Rev. 104 (2004) 4791.

[10] S. Bebelis, N. Kotsionopoulos, A. Mai, D. Rutenbeck, F. Tietz, Solid State Ionics 177 (2006) 1843.

[11] K. Zhang, L. Ge, R. Ran, Z.P. Shao, S.M. Liu, Acta Materialia 56 (2008) 4876.

[12] D.J. Chen, R. Ran, K. Zhang, J. Wang, Z.P. Shao, J. Power Sources 188 (2009) 96.

[13] G. Kim, S. Wang, A.J. Jacobson, L. Reimus, P. Brodersen, C.A. Mims, J. Mater. Chem. 17 (2007) 2500.

[14] J.H. Kim, M. Cassidy, J.T.S. Irvine, J. Bae, J. Electrochem. Soc. 156(6) (2009) B682.

[15] C.J. Zhu, X.M. Liu, C.S. Yi, D.T. Yan, W.H. Su, J. Power Sources 185 (2008) 193.

[16] M. Kleitz, F. Petitbon, Solid State Ionics 92 (1996) 65.

[17] H. Fukunaga, M. Ihara, K. Sakaki, K. Yamada, Solid State Ionics 86-88 (1996) 1179.

[18] H.P. Ding, X.J. Xue, X.Q. Liu, G.Y. Meng, J. Power Sources 195 (2010) 775.

[19] L. Zhao, B.B. He, Q. Nian, Z.Q. Xun, R.R. Peng, G.Y. Meng, X.Q. Liu, J. Power Sources 194 (2009) 291.

[20] B. Lin, S. Zhang, L. Zhang, L. Bi, H.P. Ding, X.Q. Liu, G.Y. Meng, J. Power Sources 177 (2009) 330.

[21] B. Lin, Y.C. Dong, R.Q. Yan, S. Zhang, M. Hu, Y. Zhou, G.Y. Meng, J. Power

Sources 186 (2009) 446.

[22] C.R. Xia, M.L. Liu, Solid State Ionics 152-153 (2002) 423.

[23] C.R. Xia, F.L. Chen, M.L. Liu, Electrochem. Solid-State Lett. 4(5) (2001) A52.

[24] L. Zhang, S.P. Jiang, W. Wang, Y.J. Zhang, J. Power Sources 170 (2007) 55.

Figure captions

Fig. 1. XRD patterns for (a) the pure $Ba_{0.5}Sr_{0.5}Co_2O_{5+\delta}$ (PBSC) powders calcined at 1100°C for 2h, (b) the $BaCe_{0.7}Y_{0.2}Zr_{0.1}O_{3-\delta}$ (BCYZ) powders calcined at 1100°C for 2h, and (c, d) PBSC-BCYZ composite cathodes calcined in air for 2h at 900 and 1100°C, respectively.

Fig. 2. Area-specific resistance (ASR) results for the symmetrical cells of PBSC-BCYZ sintered in air for 2h at 900, 1100 and 1200°C, respectively.

Fig. 3. Cross-section images of the post-examined symmetric cathodes. PBSC-BCYZ bulk for cathode sintered at 900°C (a) and 1200°C (b) for 2h; Cathode (PBSC-BCYZ) / electrolyte (BCYZ) interface sintered at 900°C (c) and 1200°C (d) for 2h.

Fig. 4. Performance of the single cell under humidified hydrogen atmosphere at different temperatures.

Fig. 5. Impedance spectra of the cell measured under open-circuit condidtions at different temperatures.

Fig. 6. The interfacial polarization resistances (R_p), ohmic resistances (R_o), total resistances (R_t), and the ratio of interfacial polarization resistance to total resistance (R_p/ R_t) obtained from the impedance spectra at different temperatures of the cell.

Fig. 7 Cross-section images of the post-examined single cell: (a) the cell with a 15μm-thick BCYZ membrane and (b) the PBSC-BCYZ composite cathode.

Figures

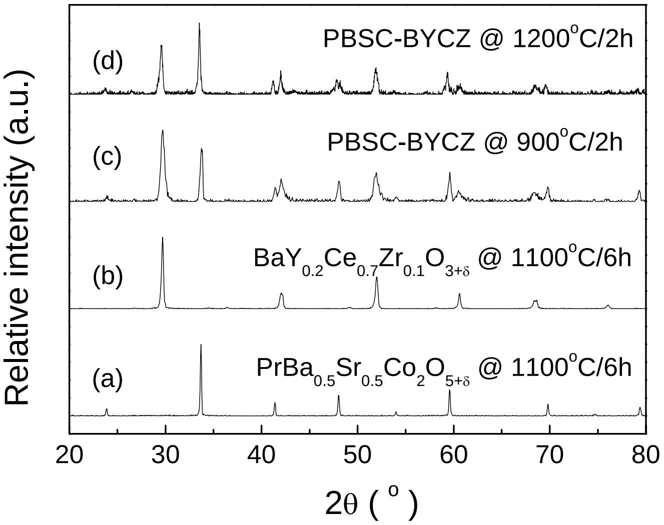

Fig. 1

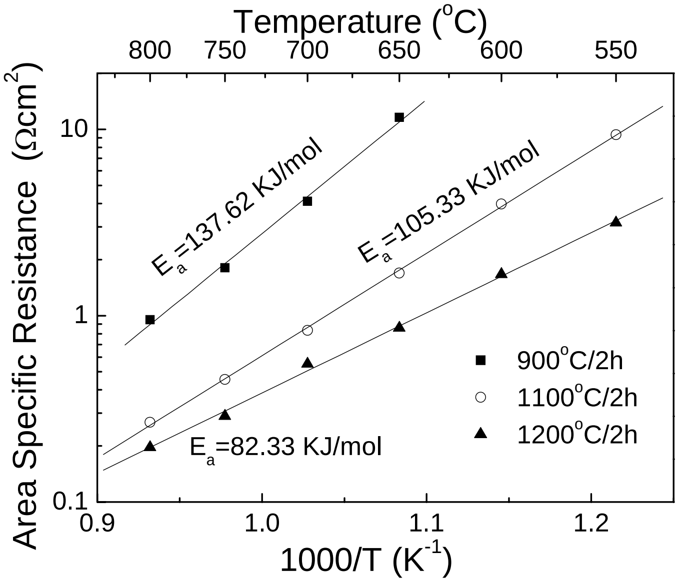
Temperature (^oC)
800
750
700
650
600
550
Area Specific Resistance (Ωcm^2)
10
1
0.1
0.9
1.0
1.1
1.2
1000/T (K^{-1})
E_a=137.62 KJ/mol
E_a=105.33 KJ/mol
E_a=82.33 KJ/mol
■ 900^{o}C/2h
○ 1100^{o}C/2h
▲ 1200^{o}C/2h

Fig. 2

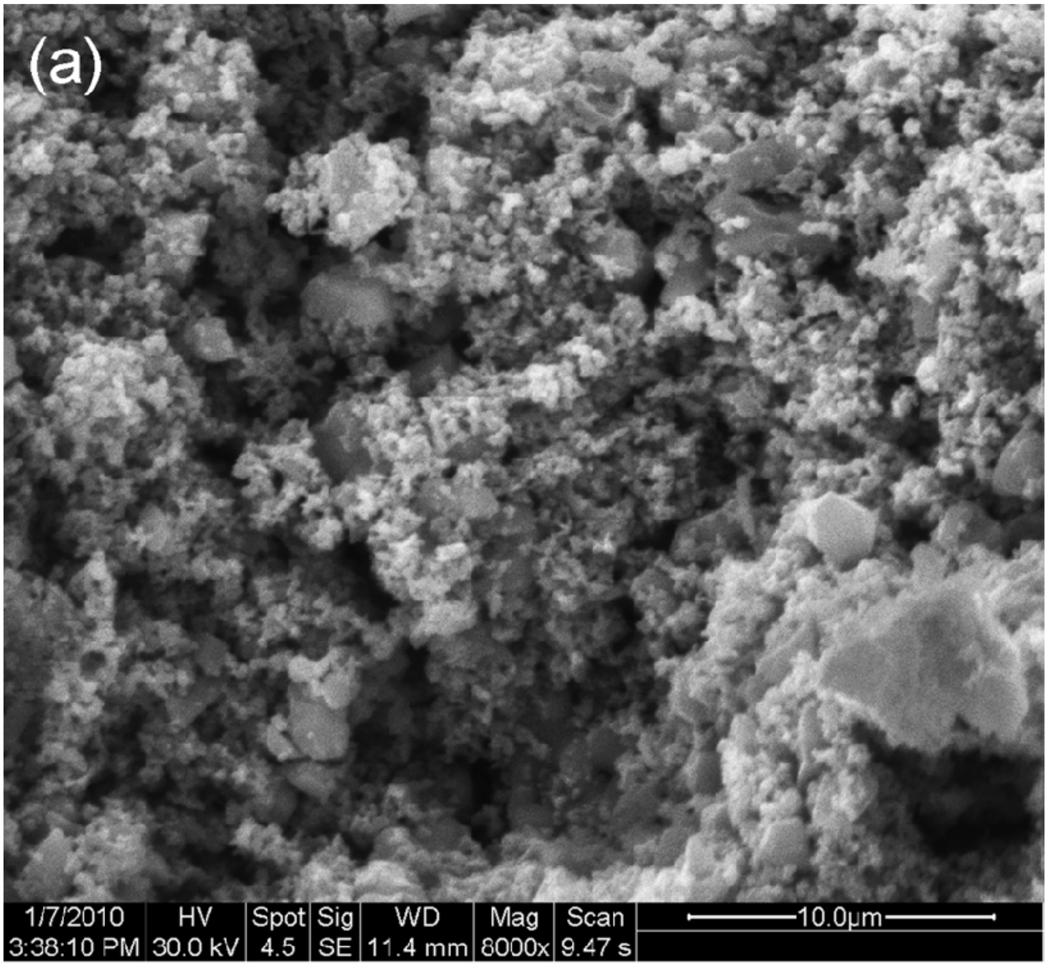
(a)
1/7/2010
3:38:10 PM
HV
30.0 kV
Spot
4.5
Sig
SE
WD
11.4 mm
Mag
8000x
Scan
9.47 s
10.0µm

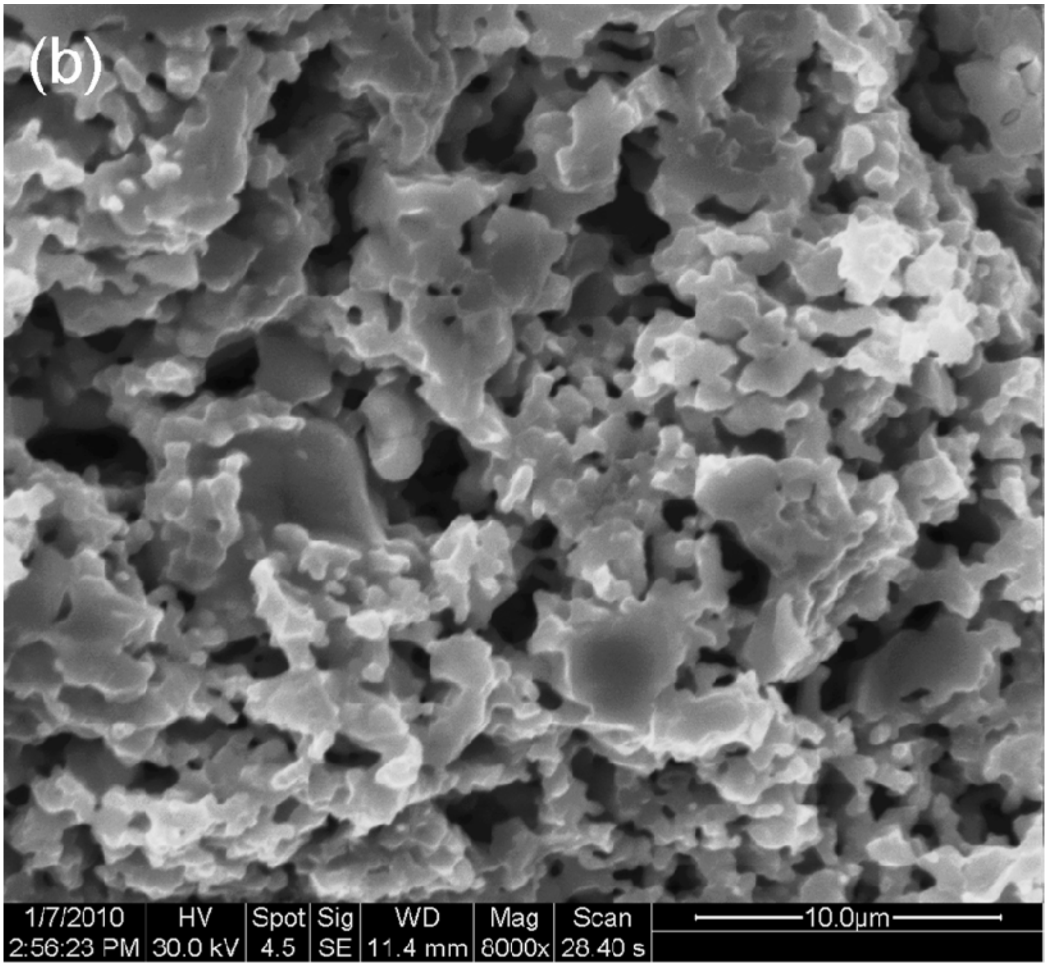
(b)
1/7/2010
2:56:23 PM
HV
30.0 kV
Spot
4.5
Sig
SE
WD
11.4 mm
Mag
8000x
Scan
28.40 s
10.0µm

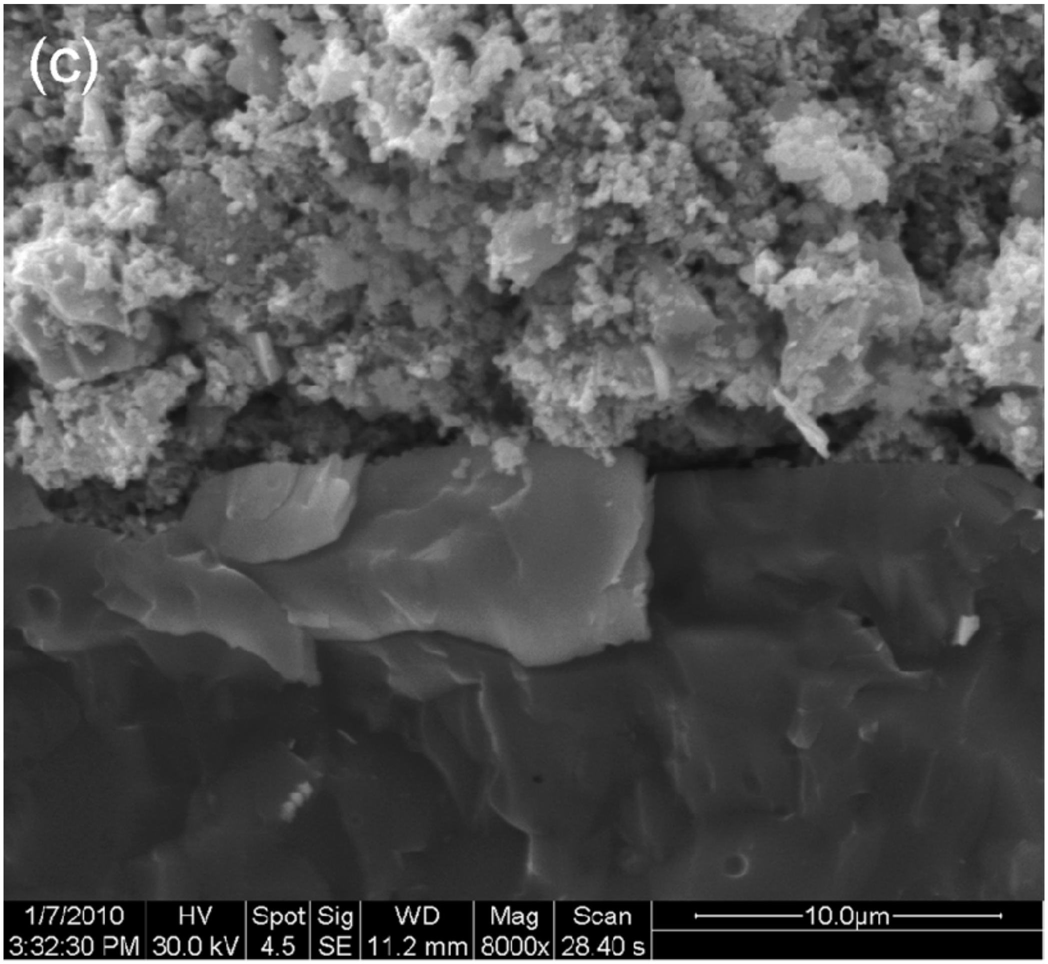
(c)
1/7/2010
3:32:30 PM
HV
30.0 kV
Spot
4.5
Sig
SE
WD
11.2 mm
Mag
8000x
Scan
28.40 s
10.0μm

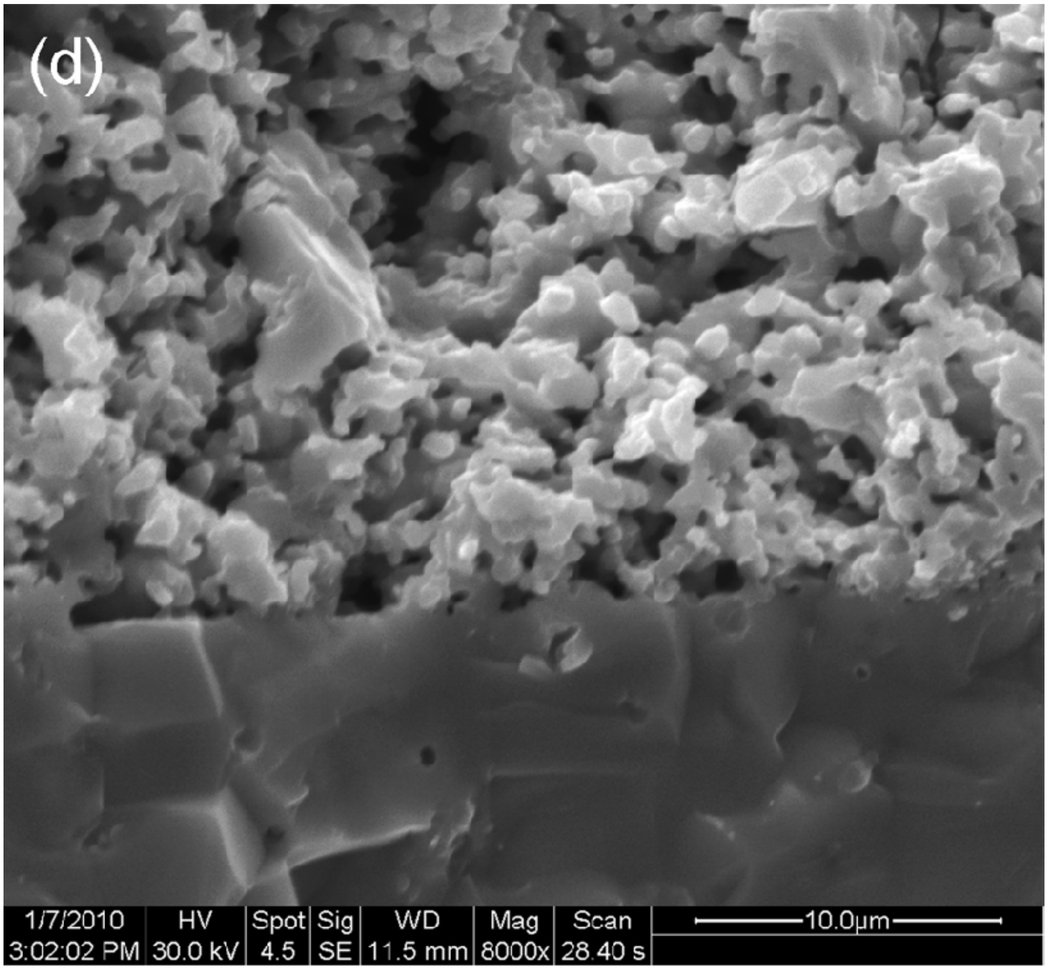
(d)
1/7/2010
3:02:02 PM
HV
30.0 kV
Spot
4.5
Sig
SE
WD
11.5 mm
Mag
8000x
Scan
28.40 s
10.0µm

Fig. 3

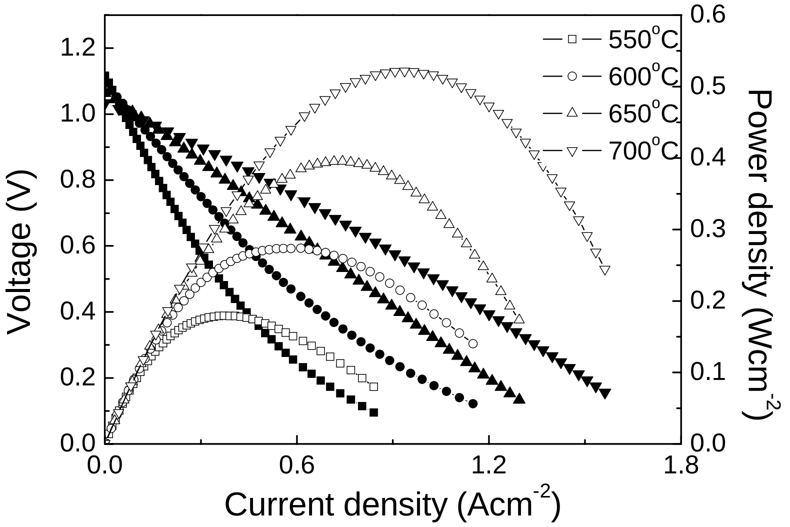

0.0
0.2
0.4
0.6
0.8
1.0
1.2
Voltage (V)
0.0
0.6
1.2
1.8
Current density (Acm^{-2})
0.0
0.1
0.2
0.3
0.4
0.5
0.6
Power density (Wcm^{-2})
550^oC
600^oC
650^oC
700^oC

Fig. 4

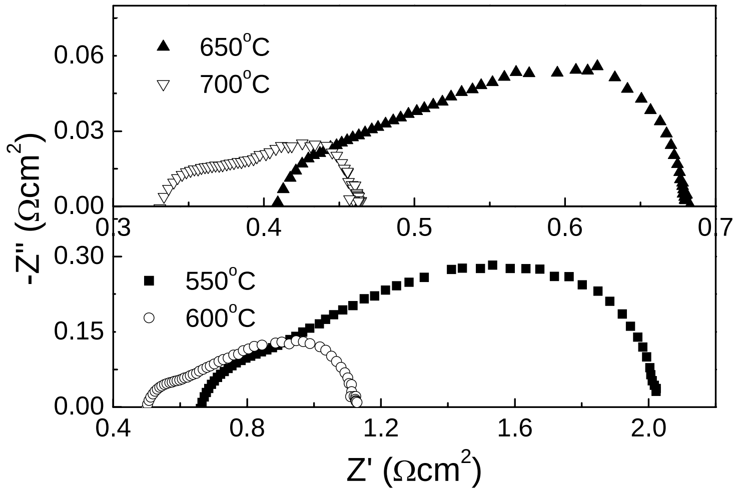
650°C
700°C
550°C
600°C
0.06
0.03
0.00
0.30
0.15
0.00
0.3
0.4
0.5
0.6
0.7
0.4
0.8
1.2
1.6
2.0
-Z'' (Ωcm2)
Z' (Ωcm2)

Fig. 5

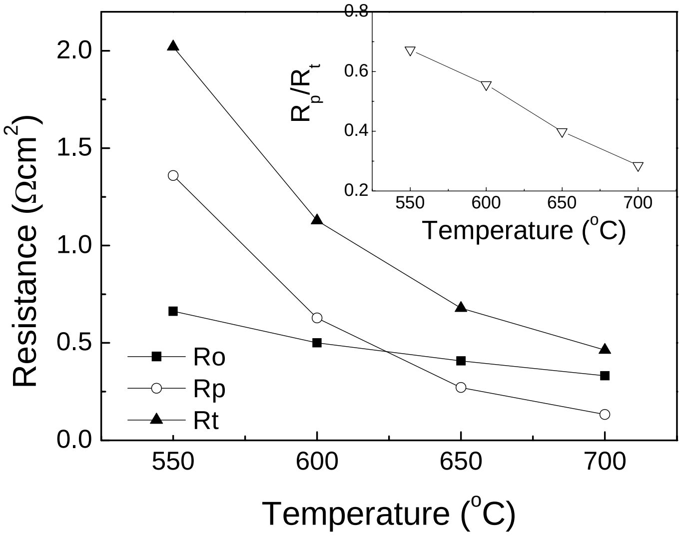
Resistance (Ωcm^2)
2.0
1.5
1.0
0.5
0.0
550
600
650
700
Temperature (^{o}C)
Ro
Rp
Rt
R_p/R_t
0.8
0.6
0.4
0.2
550
600
650
700
Temperature (^{o}C)

Fig. 6

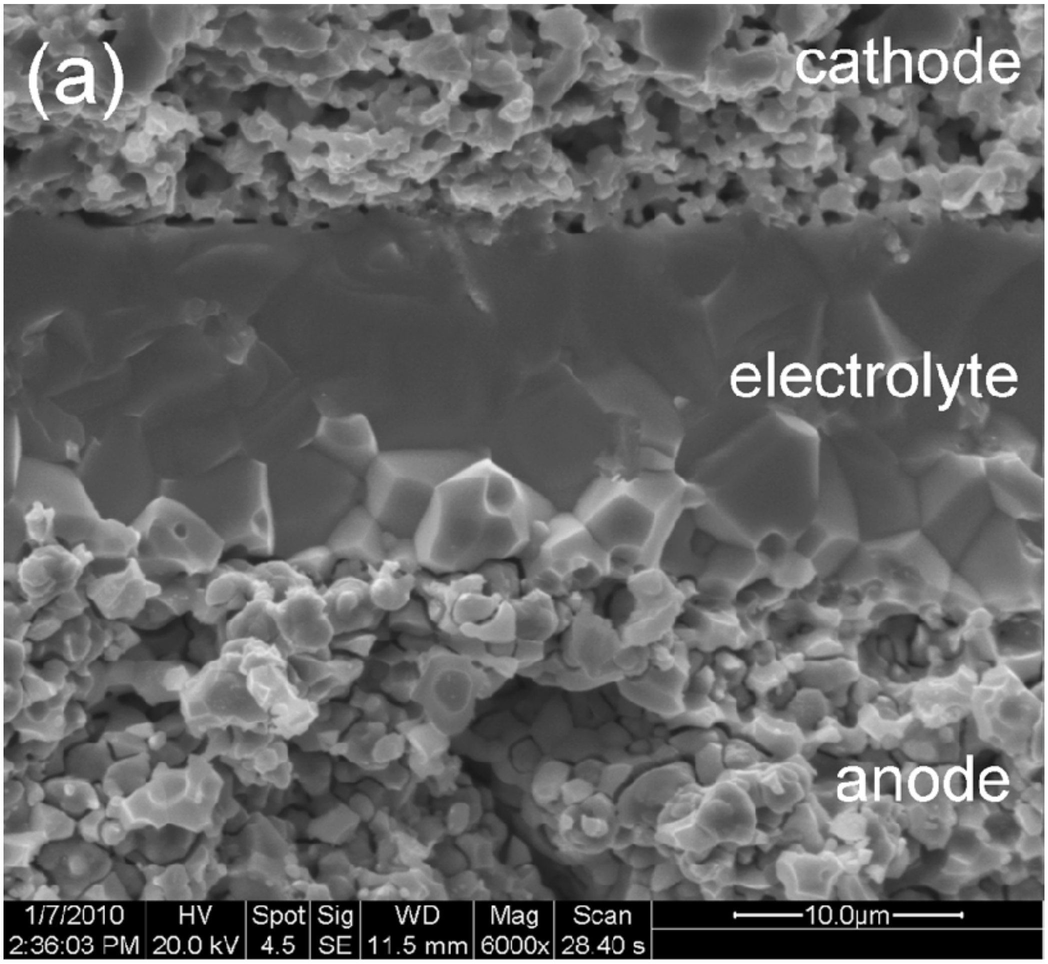
(a)
cathode
electrolyte
anode
1/7/2010 2:36:03 PM
HV 20.0 kV
Spot 4.5
Sig SE
WD 11.5 mm
Mag 6000x
Scan 28.40 s
10.0µm

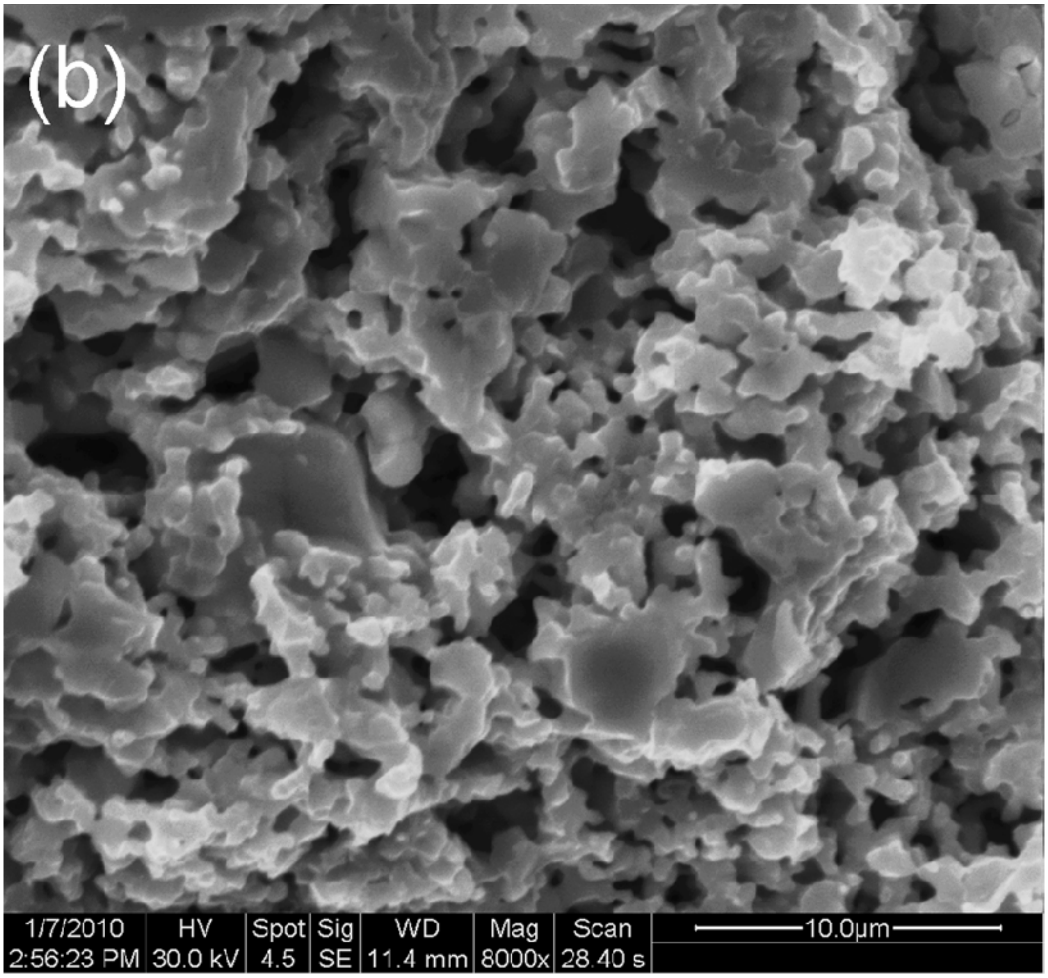
(b)
1/7/2010
2:56:23 PM
HV
30.0 kV
Spot
4.5
Sig
SE
WD
11.4 mm
Mag
8000x
Scan
28.40 s
10.0µm

Fig. 7